HHS Public Access

Author manuscript

Cancer Cell. Author manuscript; available in PMC 2016 November 09.

Published in final edited form as:

Cancer Cell. 2015 November 9; 28(5): 610–622. doi:10.1016/j.ccell.2015.09.008.

Erythropoietin Stimulates Tumor Growth *via* EphB4

Sunila Pradeep[1,*], **Jie Huang**[1,*], **Edna M. Mora**[2,3,4,*], **Alpa M. Nick**[1], **Min Soon Cho**[5], **Sherry Y. Wu**[1], **Kyunghee Noh**[1], **Chad V. Pecot**[6], **Rajesha Rupaimoole**[1], **Martin A. Stein**[7], **Stephan Brock**[7], **Yunfei Wen**[1], **Chiyi Xiong**[8], **Kshipra Gharpure**[1], **Jean M. Hansen**[1], **Archana S. Nagaraja**[1], **Rebecca A. Previs**[1], **Pablo Vivas-Mejia**[2], **Hee Dong Han**[1,9], **Wei Hu**[1], **Lingegowda S. Mangala**[1,9], **Behrouz Zand**[1], **Loren J. Stagg**[10], **John E. Ladbury**[10], **Bulent Ozpolat**[11], **S. Neslihan Alpay**[11], **Masato Nishimura**[1], **Rebecca L. Stone**[1], **Koji Matsuo**[1], **Guillermo N. Armaiz-Peña**[1], **Heather J. Dalton**[1], **Christopher Danes**[1], **Blake Goodman**[1], **Cristian Rodriguez-Aguayo**[11], **Carola Kruger**[12], **Armin Schneider**[12], **Shyon Haghpeykar**[1], **Padmavathi Jaladurgam**[1], **Mien-Chie Hung**[13], **Robert L. Coleman**[1], **Jinsong Liu**[14], **Chun Li**[10], **Diana Urbauer**[15], **Gabriel Lopez-Berestein**[9,11], **David B. Jackson**[7], and **Anil K. Sood**[1,9,16]

[1]Department of Gynecologic Oncology, The University of Texas MD Anderson Cancer Center, Houston, TX 77584

[2]Department of Surgery, School of Medicine, University of Puerto Rico, San Juan, Puerto Rico

[3]University of Puerto Rico Comprehensive Cancer Center, San Juan, Puerto Rico

[4]Department of Surgical Oncology, Chapel Hill, NC

[5]Department of Benign Hematology, Chapel Hill, NC

[6]Division of Hematology/Oncology, Chapel Hill, NC

[7]MolecularHealth GmbH, Heidelberg, Germany

[8]Department of Experimental Diagnostic Imaging, The University of Texas MD Anderson Cancer Center 77030, USA

[9]Center for RNA Interference and Non-coding RNA, The University of Texas MD Anderson Cancer Center 77030, USA

[10]Department of Biochemistry and Molecular Biology and Center for Biomolecular Structure and Function, The University of Texas MD Anderson Cancer Center, Houston, Texas 77030

[11]Department of Experimental Therapeutics, The University of Texas MD Anderson Cancer Center, Houston, Texas 77030

Correspondence: Anil K. Sood, M.D., Departments of Gynecologic Oncology and Cancer Biology, U.T. M. D. Anderson Cancer Center, 1155 Herman Pressler, Unit 1362, P.O. Box 301439 Houston, TX 77030-1439 713-745-5266 (phone), 713-792-7586 (fax), asood@mdanderson.org.

*These authors contributed equally to this manuscript.

SUPPLEMENTAL INFORMATION

Supplemental information includes Extended Procedures, supplementary figures and tables.

[12]Sygnis AG, Germany

[13]Molecular & Cellular Oncology, The University of Texas MD Anderson Cancer Center, Houston, Texas 77030, USA

[14]Department of Pathology, The University of Texas MD Anderson Cancer Center, Houston, Texas 77030, USA

[15]Biostatistics, The University of Texas MD Anderson Cancer Center, Houston, Texas 77030, USA

[16]Cancer Biology, The University of Texas MD Anderson Cancer Center, Houston, Texas 77030, USA

SUMMARY

While recombinant human erythropoietin (rhEpo) has been widely used to treat anemia in cancer patients, concerns about its adverse effects on patient survival have emerged. A lack of correlation between expression of the canonical EpoR and rhEpo's effects on cancer cells prompted us to consider the existence of an alternative Epo receptor. Here, we identified EphB4 as an Epo receptor that triggers downstream signaling *via* STAT3 and promotes rhEpo induced tumor growth and progression. In human ovarian and breast cancer samples, expression of EphB4 rather than the canonical EpoR correlated with decreased disease-specific survival in rhEpo-treated patients. These results identify EphB4 as a critical mediator of erythropoietin-induced tumor progression and further provide clinically significant dimension to the biology of erythropoietin.

INTRODUCTION

Erythropoiesis-stimulating agents (ESAs) such as recombinant human epoetin (rhEpo) and darbepoetin are recombinant glycosylated analogues of erythropoietin (Epo) that have been used to relieve chemotherapy-induced anemia in cancer patients (Glaspy, 2009a; Sytkowski, 2007). Epo is a pleiotropic cytokine that regulates erythropoiesis, angiogenesis, cytoprotection, and proliferation (Foley, 2008; Glaspy, 2009b). Alarmingly, a growing number of studies have demonstrated that ESA-based treatment can compromise overall survival of cancer patients (Crouch and DeSantis, 2009; Kumar et al., 2012; Tovari et al., 2008; Wang et al., 2011), raising the possibility of growth-stimulatory effects on cancer cells *via* the canonical Epo receptor (EpoR) (Aapro et al., 2012; Chateauvieux et al., 2011; Hedley et al., 2011; McKinney and Arcasoy, 2011; Rathod and Salahudeen, 2011). However, EpoR expression on cancer cells has largely failed to explain the effects of rhEpo on tumor growth. For example, rhEpo can affect proliferative and survival responses in cancer cells without EpoR expression (Okazaki et al., 2008), while failing to induce proliferation in EpoR-positive tumor cells (Belda-Iniesta et al., 2007). Other explanations (e.g., EpoR variants) have also been inadequate in explaining the effects of rhEpo on tumor growth (Foley, 2008).

Evidence from other therapeutic areas has also suggested the existence of an alternative Epo receptor. For example, carbamylated Epo (cEpo) does not stimulate erythropoiesis, yet prevents tissue injury in response to hypoxic conditions (Chen et al., 2009; Leist et al., 2004;

Zamora et al., 2005) in an EpoR independent manner (Leist et al., 2004). Such observations, combined with lack of a convincing molecular explanation underlying the effects of rhEpo on cancer growth prompted us to consider the existence of an alternative Epo receptor. Using a hypothesis-driven *in silico* strategy, we further explored ephrin-type B receptor 4 (EphB4) as an alternative candidate Epo receptor that accounts for many of the growth-stimulatory effects of rhEpo in tumors.

RESULTS

In silico identification of an alternative candidate Epo receptor

Epo-mediated tissue protection under conditions such as hypoxia occurs in an EpoR independent manner (Brines and Cerami, 2012; Brines et al., 2008). We reasoned that while expression of an alternative Epo receptor may mediate potential therapeutic responses to Epo under low-oxygen conditions (e.g., after ischemic stroke), expression of this same receptor on tumor cells could provide them with a survival advantage in response to Epo treatment. Such an "off-target" mechanism could have serious implications for cancer patient survival and might explain the emerging clinical evidence supporting such an effect. To identify this elusive receptor, we analyzed the membrane-bound portion of the proteome for candidate receptors possessing structural, regulatory, and functional features consistent with Epo binding, response to hypoxic conditions, and tumorigenic signaling. Employing a combination of bioinformatics and text-mining approaches, we identified EphB4, IL6rb, Tie1, Tf, and Ghr as potential candidates. While EphB4 and IL6rb showed evidence of involvement in angiogenesis and erythropoiesis, analysis of the *Epo* genomic locus revealed that it is contiguous to the *EPHB4* gene, a phenomenon not uncommon to many functionally interacting proteins (Figure S1A). Subsequent structural analyses identified potential Epo binding sites on EphB4, leading us to select this molecule as our prime candidate for an alternative Epo receptor (Figure1A).

We initially assessed whether rhEpo binds to EphB4 using fluorescence microscale thermophoresis (MST) and surface plasmon resonance (SPR). MST experiments with fluorophore labeled rhEpo demonstrated binding to EpoR with an apparent dissociation constant ($K_{D,app}$) of 28.0 ± 14.0 nM (Figure 1B) and EphB4 with a $K_{D,app}$ value of 880.6 ± 128.6 nM; Figure 1C). EphB4 and EphrinB2 bound with a $K_{D,app}$ value of 140.5 ± 28.3 nM (Figure 1D). The BSA control showed no binding to EpoR or EphB4 (Figures S1B and S1C). SPR studies revealed that rhEpo competes with EphrinB2 for EphB4 in a dose-dependent manner (Figures 1E and 1F). Controls showed EphrinB2 binding to EphB4 and rhEpo binding to EpoR (Figures S1D and S1E). A ligand with lower binding affinity can bind to its corresponding receptor and exert biological functions (Figure S1F). To test the specificity of rhEpo binding to EphB4, we also tested several other Eph receptors. No binding was noted between rhEpo and EphA2, EphA3 or EphB2 (Figure S1G-S1I); for controls, we used EphrinA1 as the ligand for EphA2, EphrinB2 for EphB2, and EphrinA2 for EphA3. Presence of rhEpo did not interfere with the binding of these ligands to their corresponding receptors (Figure S1J-L). Both rhEpo-alpha and rhEpo-beta also bind to EphB4 (50 ng/mL) in the presence of [I^{125}] rhEpo (Figures S1M and S1N).

Next, we examined a panel of cell lines for EpoR, EphB4, and EphrinB2 expression (Figure S1O-S1Q). EphrinB2 is present in endothelial cells both *in vitro* and *in vivo*, but no significant increase in its expression was observed after rhEpo stimulation (Figure S1R-S1U). The A2780 cells express both EpoR and EphB4, but lack EphrinB2 (Figures S1O-S1Q) and IL6rb (Figures S1V and S1W). To confirm specificity of the EpoR antibody, we ectopically expressed HA tagged EpoR in A2780 cells and detected EpoR expression using HA antibody (Figure S1X).

rhEpo binds to EphB4

Next, we established stably transfected clones with shRNA against EpoR (shEpoR), EphB4 (shEphB4) or both in A2780 cells (Figure S2A-S2D). ShEpoR clone 3 and shEphB4 clone 1 were used for subsequent experiments. rhEpo competitively inhibited [I^{125}]rhEpo binding to A2780-shEpoR and A2780-shEphB4 cells (Figure 2A); there was no binding of [I^{125}]rhEpo to A2780-shEpoR/shEphB4 cells (Figure 2B). To further examine the potential for EphB4 binding to Epo, we also generated $EpoR^{-/-}$ MEFs (EphB4 positive) from $EpoR^{-/-}$ mice and found that [I^{125}]rhEpo can bind to these cells (Figure 2C).

To further examine binding between Epo and EpoR or EphB4, we ectopically expressed EpoR or EphB4 in EpoR/EphB4-null Cos-1 cells. rhEpo competitively inhibited [I^{125}]rhEpo binding to both clones (Figure S2E and Table S2) and no binding was noted in Cos-1-EV (empty vector) cells. To test the specificity of shRNA, additional clones were tested with similar results obtained (Figure S2F). Similar binding patterns were also noted in MDA-MB231 (Figure S2G) and MCF-7 breast cancer cells (Figure S2H). Next, we designed several peptides from the EphB4 extracellular domain based on potential interaction sites from the 3D structures of EphB4:EphrinB2 and EpoR:Epo complexes (Figure S2I;). In competitive binding assays with rhEpo and each peptide (Figure 2D; Figure S2J), only the EEL peptide (amino acids 43-58 of the EphB4 extracellular domain covers the C-D loop (Chrencik et al., 2006a), a region involved in Ephrin-binding) inhibited the binding of [I^{125}]-rhEpo to A2780-shEpoR cells. Alignment of the N-terminal domains of EphB4 and EpoR indicated that the EEL peptide contains several residues that are identical or similar to residues in the A-B loop of EpoR, which are involved in Epo binding (Syed et al., 1998). We designed specific plasmids encoding EphB4 with a mutation at the EphrinB2 binding domain. The mutation site corresponds to the amino acids included in the EEL peptide: Ser46, Leu48, Glu50, Glu44 and Tyr58 (Table S1) (Chrencik et al., 2006a; Chrencik et al., 2006b). The Ser46 mutated site did not affect rhEpo binding, but mutations in Leu48 blocked rhEpo binding (Figure S2K and Table S2). We also mutated shared residues (Glu50 or Glu44, Tyr58) involved in Epo binding in both EphB4 and EpoR; mutation on Glu44 or Glu50 (but not Tyr 58) interrupted the binding of Epo to EphB4 (Figure S2L and Table S2). Using proximity ligation assays, we found that Epo and EphB4 interact directly in Cos-1/EpoR and Cos-1/EphB4 cells (Figure 2E-2F).

Next, we performed competitive binding studies where A2780-shEpoR cells were exposed to soluble EphB4, EphrinB2, or EpoR. Soluble EpoR did not inhibit the interaction between rhEpo and EphB4, however, soluble EphB4 and soluble EphrinB2 blocked this interaction (Figure 2G). In A2780-shEphB4 cells, soluble EpoR competitively inhibited rhEpo binding

to EpoR, but soluble EphB4 and soluble EphrinB2 did not block the interaction between rhEpo and EpoR (Figure S2M). To test the specificity of competitive inhibition, we performed assays using IL3 [known to form heterodimers with EpoR (Krosl et al., 1996)] and CXCL12 (unrelated to EpoR), and no inhibition was noted (Figure S2N).

Epo-mediated EphB4 activation and signaling

Serum rhEpo levels of 1-200 IU/mL in individuals given rhEpo have been reported (McMahon et al., 1990; Olsson-Gisleskog et al., 2007), but no data regarding levels in the tumor microenvironment were found. Thus, we evaluated human and murine Epo levels in A2780 tumors from mice treated with rhEpo (Figure S3A-D). Hemoglobin levels increased with rhEpo treatment, but there were no effects on white blood cells or platelet counts (Figure S3E). On the basis of these data, we used 1-50 IU/mL rhEpo for subsequent *in vitro* experiments. To test whether rhEpo activates EphB4, we exposed A2780, SKOV3, and MDA-MB231 cells to rhEpo. Epo and EphB4 bind to each other in a sustained manner (Figure S3F), leading to phosphorylation of EphB4 (Figure 3A; Figure S3G). To address whether cross-activation between EpoR and EphB4 could occur upon rhEpo stimulation, we immunoprecipitated EpoR and probed for EphB4 in A2780 parental cells, but no direct interaction was detected (Figure S3H). *EPHB4* mRNA levels showed modest changes in cell cycle phases in two out of four cell lines tested. To further confirm this, A2780 and MDA-MB231 cells were labeled with EphB4 antibody and FACS sorted according to cell cycle. Our data show that there were no significant change in EphB4 protein expression during different phases of the cell cycle (Figure S3I).

As expected, rhEpo stimulation of A2780-shEphB4 cells, but not A2780-shEpoR cells, resulted in activation of the Jak2/STAT5 pathway (Figure 3B). In contrast, rhEpo stimulation of A2780-shEpoR, but not A2780-shEphB4 cells, resulted in STAT3 activation (Figure 3B and Figure S3J). To further exclude the possible effect of EpoR in these experiments, we used $EpoR^{-/-}$ MEFs, which are EphB4 positive (Figure S3K). We stimulated the $EpoR^{-/-}$ MEFs with rhEpo and this resulted in increased pSTAT3 and pSrc levels (Figure 3C). Similarly, EphrinB2 treatment also resulted in STAT3 and Src phosphorylation (Figure S3L). Immunoprecipitation (IP) of EphB4 followed by immunoblotting (IB) for STAT3 revealed no evidence of direct binding between these proteins (data not shown). We then evaluated Src as a possible mediator between EphB4 and STAT3. Src IP followed by EphB4 IB revealed binding of these two proteins in A2780-shEpoR cells after rhEpo stimulation (Figure 3D). There was no binding between EphB4 and Jak2. In A2780-shEpoR cells, PP2 (Src inhibitor), but not PP3 (inactive), treatment resulted in blockage of rhEpo-induced STAT3 activation (Figure 3E). Similar results were noted with Src siRNA (Figure 3E and Figure S3M). To determine whether activated STAT3 binds to DNA upon exposure to rhEpo, we used a consensus oligonucleotide containing a binding site for STAT3. rhEpo treated A2780-shEpoR, but not the -shEphB4 cells, had >3-fold increase in nuclear STAT3 levels compared to untreated cells (Figure 3F). To further document the functionality of cellular EphB4, A2780-shEpoR cells were exposed to EphrinB2-Fc, which resulted in EphB4, Crk/Abl, and Akt phosphorylation (Figure S3N). We further confirmed this result in the $EpoR^{-/-}$ MEFs (Figure S3O).

rhEpo induces EphB4-mediated functional effects *in vitro*

Exposure to rhEpo resulted in a significant increase in proliferation, migration, and invasion of the A2780 parental and -shEpoR cells, but not A2780-shEphB4 cells (Figures 4A-C and S4A-C). Given the activation of STAT3 signaling in response to rhEpo in A2780-shEpoR cells, we examined the effects of STAT3 silencing on these cells (Figure S4D). STAT3 siRNA blocked Epo-induced proliferation (Figure S4E), migration, and invasion of A2780-shEpoR cells (Figure 4D). EphrinB2 also increased invasion, migration, and proliferation of the A2780 parental and -shEpoR cells, but not the -shEphB4 cells (Figure S4F and S4G); these effects were disrupted by STAT3 or Src siRNA (Figure S4H). EphrinB2 levels are not increased in response to rhEpo treatment (Figure S4I). Similar effects of rhEpo were noted in the MCF7 breast cancer cells using EpoR or EphB4 targeted siRNA (Figure S4J). Moreover, rhEpo increased proliferation, migration, and invasion of Cos-1 cells transfected with EphB4. These effects did not occur in Cos-1 cells expressing EpoR or mutated EphB4 (Figures S4K-M).

rhEpo induces EphB4-mediated biological effects *in vivo*

Significant increases in tumor growth following rhEpo treatment (Figures 5A and S5A) were noted in the SKOV3ip1, A2780, and HeyA8 ovarian cancer mouse models. Using fluorescently labelled (Alexa Flour 555) rhEpo, we confirmed the accumulation of rhEpo in tumors (Figure S5B). rhEpo administration increased the level of EphB4 phosphorylation in tumors (Figure S5C). Additional experiments revealed that rhEpo stimulated *in vivo* growth of A2780-shControl and -shEpoR cells, but not -shEphB4 or -shEpoR/shEphB4 cells (Figure S5D). Given the limitations of shRNA for therapeutic applications, we also used siRNA packaged in DOPC nanoliposomes for systemic siRNA delivery to tumors (Ahmed et al., 2010; Halder et al., 2005) (Merritt et al., 2008). rhEpo treatment increased tumor growth in the A2780 tumors treated with DOPC alone or control siRNA-DOPC treatment groups (Figure S5E). While EpoR siRNA-DOPC had no effect on rhEpo-stimulated tumor growth, EphB4 siRNA-DOPC or combined EphB4/EpoR siRNA-DOPC completely abrogated rhEpo induced tumor growth (Figure 5B, Figure S5F and S5G). To exclude potential off-target effects, we tested three additional EphB4 siRNA sequences. All three sequences inhibited rhEpo induced tumor growth in the A2780 model *in vivo*. (Figure S5H). Moreover, Cos-1 cells, which do not express EpoR or EphB4, were transfected with either WT EphB4 or a mutated EphB4 plasmid carrying a non-sense mutation at the EphB4 siRNA target site. Cells transfected with WT EphB4 exhibited decreased EphB4 expression following EphB4 siRNA transfection, whereas cells with mutated EphB4 had no changes in *EPHB4* expression (Figure S5I). Consistent with *in vitro* findings, STAT3 siRNA-DOPC also blocked rhEpo stimulated growth in the A2780-shEpoR model (Figure S5J). Similar effects were noted with the MDA-MB231 (ER-negative; Figure 5C) and MCF-7 (ER-positive; Figure S5K) breast cancer models. Moreoever, in the RMG2 ovarian cancer model ($EpoR^{+}/EphB4^{-}$), rhEpo had no significant effect on tumor growth (Figure S5L). Next, we ectopically expressed WT EphB4 or the mutated form of EphB4 that does not bind to Epo in the RMG2 (EphrinB2 negative) cells; while rhEpo stimulated the growth of RMG2-EphB4 tumors (WT), it had no effect on the RMG2-EphB4 mutated model (Figure 5D and Figure S5M). Protein assessment of A2780 tumors harvested at the end of the experiment revealed

>90% EpoR or EphB4 gene silencing in the respective groups (Figure S5N). Effects of EpoR or EphB4 silencing on downstream signaling were also found to be consistent with the aforementioned *in vitro* findings (Figure S5N).

To determine the effect of rhEpo on cancer cell invasion *in vivo*, we analyzed H&E sections from rhEpo-treated A2780-shEpoR tumors. These results show that rhEpo administration led to a more invasive phenotype characterized by infiltration of tumor deeply through the muscle layers, while tumors in untreated mice remained encapsulated (Figures S5O and S5P).

We next used the SKOV3ip1 (EphrinB2 negative) model to examine potential effects of endogenous EphrinB2 on murine cells. For this experiment, we used RGD-labeled chitosan (CH) nanoparticles that are highly efficient for targeted siRNA delivery (Han et al., 2008; Pradeep et al., 2014; Rupaimoole et al., 2014; Wu et al., 2014). Tumor-bearing animals were randomized to: 1) Control siRNA; or 2) human EpoR siRNA (hEpoR siRNA) and mouse EphrinB2 siRNA (mEphrinB2 si). rhEpo stimulated tumor growth in both groups (Figure S5Q and S5R). To exclude the potential effects of murine EphrinB2 on EphB4 receptor in tumor cells, we performed an additional experiment where ID8VEGF ($EphrinB2^{-}$/$EpoR^{-}$/$EphB4^{+}$) cells were injected i.p. into EphrinB2 KO mice (Figure 5E, Figure S5S and S5T). We found that rhEpo still promotes tumor growth in this model.

EphB4 expression correlates with clinical outcome in ESA-treated patients

Next, we addressed potential effects of tumoral EpoR or EphB4 expression on the effects of ESA treatment in patients with ovarian (n = 175) or breast (n = 88) cancer (Figure 6A-D and Figure S6A-C). EphB4 and EpoR protein levels were significantly correlated with mRNA expression levels (Figure S6D and S6E). The mean age of the patients with epithelial ovarian cancer was 58.2 years (range, 20-92 years); 85% had serous histology, and 91% had high-grade tumors. All patients were primarily treated with combination platinum and taxane chemotherapy. EpoR and EphB4 overexpression was detected in 79% and 39% of epithelial ovarian cancer samples, respectively (Tables S3). The disease-specific survival (DSS) in patients with high EphB4-expressing tumors was significantly shorter than for patients with low EphB4-expressing tumors ($p<0.001$; Figure 6E; Table S4). DSS did not differ by level of EpoR expression (Figure 6F; $p=0.64$; Table S4). In multivariate analysis, EphB4, but not EpoR overexpression was an independent predictor of poor survival (Table S4). High level of EphB4 expression, but not EpoR, was associated with shorter overall patient survival compared to low EphB4 expression ($p < 0.001$; Figure 6G).

Next, we addressed the potential impact of ESA-based treatment on survival of patients with ovarian cancer. ESA-based treatment was associated with shorter survival in patients with EphB4-overexpressing tumors (2.18 *versus* 4.52 years; $p=0.0004$), but not in patients with low EphB4-expressing tumors (4.38 *versus* 5.28 years; $p=0.19$; Figure 6H). To determine if EphB4 interacts with ESA-based treatment to adversely impact outcomes, a Cox proportional hazards model was created (Table S4). In this model, patients with high EphB4 expression and ESA-treatment had increased risk of disease-specific mortality than those with low EphB4 and no ESA-therapy (HR 5.66 (95% CI 3.11-10.31), $p<0.0001$). In contrast, patients with low EphB4 and ESA-therapy did not demonstrate a similar relationship (HR

0.88 (95% CI 0.45-1.74), p=0.71). ESA-therapy was associated with worse survival in patients with low EpoR expression (p=0.03, Figure S6F). To determine the specificity of the ESA and EphB4 interaction, a parallel analysis was performed with IL6rb, one of the other candidates identified in the *in silico* screen; there was no impact on patient survival based on IL6rb expression (Figure S6G-S6I).

To determine whether EphB4 expression is predictive of outcome in patients with other malignancies, we also tested breast cancer samples (n=88; further details included in Tables S5 and S6). DSS of ESA-treated breast cancer patients was significantly lower compared to untreated patients (Figure 6I). ESA-treated breast cancer patients with high EphB4 expression showed significantly lower survival compared to untreated patients (Figure 6J). For those with available Her2 and estrogen receptor status, ESA treatment was associated with increased risk of death (HR: 4.09; 95% CI=1.32-12.68). After stratifying patients according to receptor status, those with Her2 negative tumors had an increased risk of death with ESA therapy (HR: 10.3; 95% CI=1.07-98.76; Table S7). Collectively, we propose a model whereby Epo interacts with the EphB4 receptor, leading to downstream Src and STAT3 activation (Figure 7).

DISCUSSION

This study identified EphB4 as a previously unrecognized Epo receptor that is responsible for the deleterious effects of exogenous Epo administration on the survival of cancer patients. The computational, biochemical, molecular, cellular, animal, and clinical data support the role of EphB4 as a functional Epo receptor.

Administration of exogenous Epo in patients with cancer has been linked with tumor progression (Crouch and DeSantis, 2009; Kumar et al., 2012; Tovari et al., 2008; Wang et al., 2011), but the mechanism remained elusive until now. Although the interaction between Epo and the canonical EpoR can explain tumor progression in some models, mounting evidence indicates that this interaction is not involved in most Epo-induced tumor growth (Sturm et al., 2010 and Kassem and Yassin, 2010). A possible explanation to this puzzle is the concept that alternative EpoRs (e.g. EpoR–IL3 heterodimer and soluble EpoR) can account for non-hematological effects, but these alternative receptors have not explained Epo-induced tumor progression. Our results have broad implications for understanding Epo biology. For example, the Epo-EphB4 pathway could potentially explain some of the non-hematologic functions of Epo. EphB4 is present, and tends to colocalize with EpoR in a subset of cortical neurons (Figure S6J) (Uhlen et al., 2015). Pharmacological doses of cEpo have neuroprotective effects that have been shown to be independent of EpoR function (Sturm et al., 2010). Epo has been shown to prevent chemotherapy-induced neurotoxicity in cancer patients (Kassem and Yassin, 2010). Administration of Epo after a stroke can reduce the extent of damage and accelerate patient recovery (Chang et al., 2005; Noguchi et al., 2007).

EphB4 appears to be a low affinity receptor for rhEpo based on the biochemical data. The concentration of rhEpo used for the biological experiments (50 IU/ml) corresponds to 10-15 nM, which is 1% to 2% of the K_D value (K_D=881nM) for the binding of rhEpo to EphB4, as

measured in the MST assay. These data suggest that as a relatively low-affinity binding event, interaction between rhEpo and EphB4 is a pharmacologically efficient process. Other ligand-receptor systems that display similar phenomena have been reported previously (Authier and Desbuquois, 2008; Hutchinson et al., 2003; Mason and Tager, 1985). Whether EphB4 exists as a dimer in cancer cells is not known and will require additional work. Our findings can also be extrapolated to the mechanism by which Epo could potentially induce neovascularization in normal organs (Davies et al., 2009; Salvucci et al., 2006), a process also regulated by EphB4.

The discovery of EphB4 as an alternative Epo receptor has multiple clinical implications including opportunities for patient stratification, and anti-EphB4 approaches to abrogate the stimulatory effects of Epo on tumor growth. In summary, Epo-EphB4 interactions on tumor cells provide a previously unrecognized dimernsion for our understanding of Epo-mediated tumor growth.

EXPERIMENTAL PROCEDURES

Animal model Studies

Female athymic nude mice (NCr-nu) and immunocompetent (C57BL/6) mice (5–8 weeks) were purchased from the NCI-Frederick Cancer Research and Development Center (Frederick, MD). B6;129S-Eportm1Liz/J and B6.129S7-Efnb2tm2And/J mice were purchased from Jackson Laboratory and maintained as previously described (Merritt et al., 2008b; Thaker et al., 2006). All animal work was performed in accordance with protocols approved by the M.D. Anderson Institutional Animal Care and Use Committee. Mice were cared for in accordance with guidelines set forth by the American Association for Accreditation of Laboratory Animal Care and the US Public Health Service Policy on Human Care and Use of Laboratory Animals.

MST experiments were performed using a NanoTemper NT.115 Monolith system (Jerabek-Willemsen et al., 2011). Temperature was maintained at 25°C for all experiments. Purified, recombinant proteins were obtained from Cell Sciences (epoetin) and Sino Biological (EpoR, EphB4, and EphrinB2/Fc). Fluorescence labeling of rhEpo and EphB4 was achieved through primary amide coupling with NT-647 dye (NanoTemper), and labeled protein was purified from free dye using Sephadex G25 resin (GE Healthcare). The concentration of NT-647 labeled protein was maintained at 25 nM throughout and titration series of unlabeled protein were accomplished with dilution in assay buffer (10 mM HEPES, pH 7.5, 150 mM NaCl, 0.5 mM TCEP, 0.05% Tween-20). Individual samples were made up to ≤5 μl in standard, glass capillaries (NanoTemper). A thermal gradient of ~3°C produced the characteristic thermophoretic trace for each sample. Each data point represents the average of triplicate repeats, and reported error is the standard deviation of triplicate repeats. Data were analyzed using NanoTemper software. Affinities calculated near the concentration of labeled protein (25 nM) are denoted $K_{D,app}$ as a higher inherent error is expected.

Surface plasmon resonance (SPR): Immobilization of EphB4 receptor to sensor chip

The stock solution (100 μg/mL) of EphB4 in phosphate-buffered saline (PBS) was diluted to 25 μg/mL with 10 mM sodium acetate buffer at pH 4.5 and immobilized to a CM5 sensor chip using the amine coupling reaction following manufacturer-provided procedures (BIACORE). Briefly, the surfaces of the chips in flow cells (FC)-1, -2 were activated by exposing them to a mixture of 200 mM *N*-ethyl-*N'*-dimethylaminopropyl carbodiimide and 50 mM *N*-hydroxysuccinimide for 7 min. FC-1 was used as a reference surface and was directly deactivated by injecting 1 M ethanolamine at pH 8.5 for 7 min. FC-2 was injected with 25 μg/mL EphB4, followed by injection of 1 M ethanolamine to block the remaining activated ester groups on the surface. The chip was allowed to stabilize for at least 2 h in HBSEP running buffer before injecting test analytes. The experiments were performed in triplicate.

SPR Binding assays between EphrinB2 and EphB4

Binding assays were performed in triplicate at 25 °C in HBSEP running buffer. EphrinB2 was diluted in HBSEP buffer, filtered, degassed, and injected at concentrations between 0.6 nM and 40 nM at a flow rate of 30 μl/min. The injection time of EphrinB2 into the HBSEP buffer was 7 min, followed by a 3-min dissociation period. The chips were regenerated using a 30 s pulse of 10 mM glycine (pH 2.2) after each binding circle. Each cycle consisted of a 2-min waiting period to allow monitoring of the baseline binding stability. For subtraction of bulk effects, caused by changes in the buffer composition or nonspecific binding, we performed double-referencing. Therefore, all analyzed samples were additionally injected onto an uncoated reference surface, including a sample of the running buffer, which was also tested on the EphB4 coated flow cell.

Competition of rhEpo and EphrinB2 for EphB4 receptor

The ability of rhEpo to inhibit EphrinB2 binding to EphB4 was assessed in a competitive binding assay. Serial dilutions of rhEpo from 0.39 to 100 nM were mixed with a predetermined concentration of EphrinB2 (2.5 nM) in HBSEP buffer containing 0.1 mg/mL BSA to prevent nonspecific binding. The mixture was injected at a flow rate of 30 μl/min over an EphB4-coated flow cell as well as over a control flow cell. After each injection, the signal from the control flow cell was subtracted, and then the relative amount of protein bound to EphB4 was recorded as the net response over pre-injection baseline. Regeneration was achieved with a 30 s pulse of 10 mM glycine (pH 2.2). Bound protein shown as response units (RU) was plotted as a function of Epo concentration and fit to a three-parameter non-linear regression using Graphpad Prism 5.0.

The ability of rhEpo binding to other Eph receptors was tested by competitive binding assay. To test this, tubes were coated with 100 μL of EphA2 (100 nM), EphA3 (100 nM) and EphB2 (100 nM) at 4°C. Serial dilutions of Ephr inA1, EphrinA2 and EphrinB2 from 0.01 to 100 nM were mixed with a predetermined concentration of [I^{125}] rhEpo (10 nM) in HBSEP buffer containing 0.1 mg/mL BSA to prevent nonspecific binding. Radioactivity (signal) was measured after 2 hr of incubation. The data are expressed as % of binding. The experiments were performed in triplicates.

Immobilization of monoclonal mouse anti-human IgG (Fc) antibody to sensor chip and analysis of binding between Epo and rhEpoR-Fc

The same procedure as described before was performed to coat the monoclonal mouse anti-human IgG (Fc) antibody (Biacore, BR-1008-39) on CM5 chip which is ready for capture analysis. In capture analysis, each cycle consisted of (i) capture of rhEpoR-Fc by injection of 500 μL rhEpoR-Fc over flow cell 2, (ii) 1 min stabilization time, (iii) 60 μL injection of Epo (concentration range of 13.4 nM to 107 nM in 2-fold dilution increments) over flow cells 1 and 2 with flow cell 1 as the reference flow cell, (iv) 5 min dissociation (buffer flow), (v) regeneration of anti-human IgG surface with a 120 s injection of 3M $MgCl_2$ at 50 μL/min, (vi) 1 min stabilization time before start of next cycle. Signal was monitored as flow cell 2 minus flow cell 1. All samples and a buffer blank were injected in duplicate.

Clinical Samples

After informed consent, data and paraffin-embedded tissue samples on 175 consecutive patients with ovarian cancer and 88 consecutive patients with breast cancer were collected according to M.D. Anderson Institutional Review Board-approved protocol. There were no significant differences in patient demographics, clinical stage, or known prognostic factors for either cohort of patients. All patients in the ovarian cancer cohort were treated with a combination of surgical cytoreduction followed by adjuvant taxane and platinum chemotherapy. Clinical samples were scored for staining with the EphB4, EpoR, and IL-6rb antibodies by a board-certified pathologist who was blinded to the clinical outcome of the patients. EphB4, EpoR and IL-6rb expression was determined semi-quantitatively by assessing the distribution of the positive cells and the staining intensity in the tumor cells, as previously described (Lu et al., 2010; Merritt et al., 2008a). An overall H-score >100 was defined as high expression and ≤100, low expression, according to the method described by McCarty *et al*. which considers both the intensity of staining and the percentage of cells stained. The expression of EpoR and EphB4 was also verified by qRT-PCR in selected patients. To test for a difference in survival by EphB4 expression, we used 175 patients with 60% in the first group (low expression) and specified median survival time of 6.7 years in low expressers and 3 years in high expressers of EphB4. We thereby expected 65 deaths among low expressers and 42 deaths among high expressers and consequently had 99% power to detect the observed difference in survival curves. A similar post-hoc power analysis was performed in the breath cohort and we had 70% power to detect the observed difference in survival curves.

Statistical analysis

Fisher exact test was used to examine associations between EphB4, EpoR and IL6rb expression and ESA treatment in human samples and clinical variables. Kaplan-Meier survival curves and log-rank tests were used to examine the association between tumor expression of EphB4, EpoR or IL6rb and patient disease-specific survival with and without ESA treatment. Multivariable analysis was performed using the Cox proportional hazards model. The data for this analysis were tested (plot of differences in log of cumulative hazard rates of test variable against time) and found to confirm to the proportional hazards assumptions. For animal experiments, 10 mice were assigned to each treatment group. This

sample size gave 80% power to detect a 50% reduction in tumor weight with 95% confidence. Mouse and tumor weights and the number of tumor nodules in each group were compared. Data are presented as mean ± S.D. Statistical comparisons between experimental groups were analyzed by unpaired Student's *t* test, and a two-tailed $p < 0.05$ was taken to indicate statistical significance. For analyzing the correlation, we used Pearson's test and the p values are indicated. We also used Mann-Whitney rank sum test as indicated. All statistical tests were two-sided. For *in vitro* studies, those with continuous variables were compared using the student *t*-test if normally distributed. Differences in variables that were not normally distributed were compared using a nonparametric test (Mann-Whitney *U* test). Again, a p value less than 0.05 was deemed statistically significant. All statistical tests were two-sided. Only two-tailed values are reported in this study.

Full Methods are described in the supplemental information.

Supplementary Material

Refer to Web version on PubMed Central for supplementary material.

ACKNOWLEDGEMENTS

We thank Carmen Cruz, Cristina Castro, and Belisa Suarez for the collection of breast tumor samples and data. We also thank Dr. Rene Nieves Alicea, Dr. Mario Quintero, Nicholas Jennings, Donna Reynolds, Francesca Diella, Drs. Ramos, and Bharat B. Aggarwal for helpful discussion and guidance; Rahul Mitra for admistrative assistance. Portions of this work were supported by the NIH (CA 109298, P50 CA083639, P50 CA098258, CA 177909, CA128797,U54CA151668, UH2 TR000943, CA 16672, U54 CA 096300), the Ovarian Cancer Research Fund, Inc. (Program Project Development Grant), the DOD (OC 120547, OC 093416), CPRIT RP110595 and RPI 20214, the RGK Foundation, the Gilder Foundation, the Judi A. Rees Ovarian Cancer Research Fund, the Chapman Foundation, the Blanton-Davis Ovarian Cancer Research Program and the Betty Anne Asche Murray Distinguished Professorship. AMN, JBM, BZ, RLS, RAP, JMH and HJD were supported by NCI-DHHS-NIH T32 Training Grant (T32 CA101642). KM was supported by the GCF/OCRF Ann Schreiber Ovarian Cancer Research grant and an award from the Meyer and Ida Gordon Foundation #2. MMKS was supported by the NIH/NICHD WRHR Grant (HD050128) and the GCF-Molly Cade Ovarian Cancer Research Grant. LJS and JEL are supported by the G. Harold and Leila Y. Mathers Charitable Foundation. S.Y.W. is supported by Ovarian Cancer Research Fund, Inc., Foundation for Women's Cancer, and Cancer Prevention Research Institute of Texas training grants (RP101502, RP101489, and RP110595).

REFERENCES

Aapro M, Jelkmann W, Constantinescu SN, Leyland-Jones B. Effects of erythropoietin receptors and erythropoiesis-stimulating agents on disease progression in cancer. British journal of cancer. 2012; 106:1249–1258. [PubMed: 22395661]

Ahmed AA, Lu Z, Jennings NB, Etemadmoghadam D, Capalbo L, Jacamo RO, Barbosa-Morais N, Le XF, Vivas-Mejia P, Lopez-Berestein G, et al. SIK2 is a centrosome kinase required for bipolar mitotic spindle formation that provides a potential target for therapy in ovarian cancer. Cancer cell. 2010; 18:109–121. [PubMed: 20708153]

Authier F, Desbuquois B. Glucagon receptors. Cellular and molecular life sciences : CMLS. 2008; 65:1880–1899. [PubMed: 18292967]

Belda-Iniesta C, Perona R, Carpeno Jde C, Cejas P, Casado E, Manguan-Garcia C, Ibanez de Caceres I, Sanchez-Perez I, Andreu FB, Ferreira JA, et al. Human recombinant erythropoietin does not promote cancer growth in presence of functional receptors expressed in cancer cells. Cancer biology & therapy. 2007; 6:1600–1605. [PubMed: 17938574]

Brines M, Cerami A. The receptor that tames the innate immune response. Molecular medicine (Cambridge, Mass). 2012; 18:486–496.

Brines M, Patel NS, Villa P, Brines C, Mennini T, De Paola M, Erbayraktar Z, Erbayraktar S, Sepodes B, Thiemermann C, et al. Nonerythropoietic, tissue-protective peptides derived from the tertiary structure of erythropoietin. Proceedings of the National Academy of Sciences of the United States of America. 2008; 105:10925–10930. [PubMed: 18676614]

Chang YS, Mu D, Wendland M, Sheldon RA, Vexler ZS, McQuillen PS, Ferriero DM. Erythropoietin improves functional and histological outcome in neonatal stroke. Pediatric research. 2005; 58:106–111. [PubMed: 15879287]

Chateauvieux S, Grigorakaki C, Morceau F, Dicato M, Diederich M. Erythropoietin, erythropoiesis and beyond. Biochemical pharmacology. 2011; 82:1291–1303. [PubMed: 21782802]

Chen J, Connor KM, Aderman CM, Willett KL, Aspegren OP, Smith LE. Suppression of retinal neovascularization by erythropoietin siRNA in a mouse model of proliferative retinopathy. Investigative ophthalmology & visual science. 2009; 50:1329–1335. [PubMed: 18952918]

Chrencik JE, Brooun A, Kraus ML, Recht MI, Kolatkar AR, Han GW, Seifert JM, Widmer H, Auer M, Kuhn P. Structural and biophysical characterization of the EphB4*ephrinB2 protein-protein interaction and receptor specificity. The Journal of biological chemistry. 2006a; 281:28185–28192. [PubMed: 16867992]

Chrencik JE, Brooun A, Recht MI, Kraus ML, Koolpe M, Kolatkar AR, Bruce RH, Martiny-Baron G, Widmer H, Pasquale EB, Kuhn P. Structure and thermodynamic characterization of the EphB4/Ephrin-B2 antagonist peptide complex reveals the determinants for receptor specificity. Structure. 2006b; 14:321–330. [PubMed: 16472751]

Crouch Z, DeSantis ER. Use of erythropoietin-stimulating agents in breast cancer patients: a risk review. American journal of health-system pharmacy : AJHP : official journal of the American Society of Health-System Pharmacists. 2009; 66:1180–1185. [PubMed: 19535656]

Davies MH, Zamora DO, Smith JR, Powers MR. Soluble ephrin-B2 mediates apoptosis in retinal neovascularization and in endothelial cells. Microvascular research. 2009; 77:382–386. [PubMed: 19232363]

Foley RN. Erythropoietin: physiology and molecular mechanisms. Heart failure reviews. 2008; 13:405–414. [PubMed: 18236154]

Glaspy J. Hematology: ESAs to treat anemia--balancing the risks and benefits. Nature reviews Clinical oncology. 2009a; 6:500–502.

Glaspy JA. Erythropoietin in cancer patients. Annual review of medicine. 2009b; 60:181–192.

Halder J, Landen CN Jr. Lutgendorf SK, Li Y, Jennings NB, Fan D, Nelkin GM, Schmandt R, Schaller MD, Sood AK. Focal adhesion kinase silencing augments docetaxel-mediated apoptosis in ovarian cancer cells. Clinical Cancer Research. 2005; 11:8829–8836. [PubMed: 16361572]

Han LY, Fletcher MS, Urbauer DL, Mueller P, Landen CN, Kamat AA, Lin YG, Merritt WM, Spannuth WA, Deavers MT, et al. HLA class I antigen processing machinery component expression and intratumoral T-Cell infiltrate as independent prognostic markers in ovarian carcinoma. Clinical cancer research : an official journal of the American Association for Cancer Research. 2008; 14:3372–3379. [PubMed: 18519766]

Hedley BD, Allan AL, Xenocostas A. The role of erythropoietin and erythropoiesis-stimulating agents in tumor progression. Clinical cancer research : an official journal of the American Association for Cancer Research. 2011; 17:6373–6380. [PubMed: 21750199]

Hutchinson SL, Wooldridge L, Tafuro S, Laugel B, Glick M, Boulter JM, Jakobsen BK, Price DA, Sewell AK. The CD8 T cell coreceptor exhibits disproportionate biological activity at extremely low binding affinities. The Journal of biological chemistry. 2003; 278:24285–24293. [PubMed: 12697765]

Jerabek-Willemsen M, Wienken CJ, Braun D, Baaske P, Duhr S. Molecular interaction studies using microscale thermophoresis. Assay and drug development technologies. 2011; 9:342–353. [PubMed: 21812660]

Kassem LA, Yassin NA. Role of erythropoeitin in prevention of chemotherapy-induced peripheral neuropathy. Pakistan journal of biological sciences: PJBS. 2010; 13:577–587. [PubMed: 21061908]

Krosl J, Damen JE, Krystal G, Humphries RK. Interleukin-3 (IL-3) inhibits erythropoietin-induced differentiation in Ba/F3 cells via the IL-3 receptor alpha subunit. The Journal of biological chemistry. 1996; 271:27432–27437. [PubMed: 8910323]

Kumar SM, Zhang G, Bastian BC, Arcasoy MO, Karande P, Pushparajan A, Acs G, Xu X. Erythropoietin receptor contributes to melanoma cell survival in vivo. Oncogene. 2012; 31:1649–1660. [PubMed: 21860424]

Leist M, Ghezzi P, Grasso G, Bianchi R, Villa P, Fratelli M, Savino C, Bianchi M, Nielsen J, Gerwien J, et al. Derivatives of erythropoietin that are tissue protective but not erythropoietic. Science (New York, NY). 2004; 305:239–242.

Mason JC, Tager HS. Identification of distinct receptor complexes that account for high-and low-affinity glucagon binding to hepatic plasma membranes. Proceedings of the National Academy of Sciences of the United States of America. 1985; 82:6835–6839. [PubMed: 2995990]

McKinney M, Arcasoy MO. Erythropoietin for oncology supportive care. Experimental cell research. 2011; 317:1246–1254. [PubMed: 21396935]

McMahon FG, Vargas R, Ryan M, Jain AK, Abels RI, Perry B, Smith IL. Pharmacokinetics and effects of recombinant human erythropoietin after intravenous and subcutaneous injections in healthy volunteers. Blood. 1990; 76:1718–1722. [PubMed: 2224121]

Merritt WM, Lin YG, Han LY, Kamat AA, Spannuth WA, Schmandt R, Urbauer D, Pennacchio LA, Cheng JF, Nick AM, et al. Dicer, Drosha, and outcomes in patients with ovarian cancer. The New England journal of medicine. 2008; 359:2641–2650. [PubMed: 19092150]

Noguchi CT, Asavaritikrai P, Teng R, Jia Y. Role of erythropoietin in the brain. Critical reviews in oncology/hematology. 2007; 64:159–171. [PubMed: 17482474]

Okazaki T, Ebihara S, Asada M, Yamanda S, Niu K, Arai H. Erythropoietin promotes the growth of tumors lacking its receptor and decreases survival of tumor-bearing mice by enhancing angiogenesis. Neoplasia (New York, NY). 2008; 10:932–939.

Olsson-Gisleskog P, Jacqmin P, Perez-Ruixo JJ. Population pharmacokinetics meta-analysis of recombinant human erythropoietin in healthy subjects. Clinical pharmacokinetics. 2007; 46:159–173. [PubMed: 17253886]

Pradeep S, Kim SW, Wu SY, Nishimura M, Chaluvally-Raghavan P, Miyake T, Pecot CV, Kim SJ, Choi HJ, Bischoff FZ, et al. Hematogenous metastasis of ovarian cancer: rethinking mode of spread. Cancer cell. 2014; 26:77–91. [PubMed: 25026212]

Rathod DB, Salahudeen AK. Nonerythropoietic properties of erythropoietin: implication for tissue protection. Journal of investigative medicine : the official publication of the American Federation for Clinical Research. 2011; 59:1083–1085. [PubMed: 22011619]

Rupaimoole R, Wu SY, Pradeep S, Ivan C, Pecot CV, Gharpure KM, Nagaraja AS, Armaiz-Pena GN, McGuire M, Zand B, et al. Hypoxia-mediated downregulation of miRNA biogenesis promotes tumour progression. Nature communications. 2014; 5:5202.

Salvucci O, de la Luz Sierra M, Martina JA, McCormick PJ, Tosato G. EphB2 and EphB4 receptors forward signaling promotes SDF-1-induced endothelial cell chemotaxis and branching remodeling. Blood. 2006; 108:2914–2922. [PubMed: 16840724]

Sturm B, Helminger M, Steinkellner H, Heidari MM, Goldenberg H, Scheiber-Mojdehkar B. Carbamylated erythropoietin increases frataxin independent from the erythropoietin receptor. European journal of clinical investigation. 2010; 40:561–565. [PubMed: 20456483]

Syed RS, Reid SW, Li C, Cheetham JC, Aoki KH, Liu B, Zhan H, Osslund TD, Chirino AJ, Zhang J, et al. Efficiency of signalling through cytokine receptors depends critically on receptor orientation. Nature. 1998; 395:511–516. [PubMed: 9774108]

Sytkowski AJ. Does erythropoietin have a dark side? Epo signaling and cancer cells. Science's STKE : signal transduction knowledge environment. 2007; 2007:pe38.

Tovari J, Pirker R, Timar J, Ostoros G, Kovacs G, Dome B. Erythropoietin in cancer: an update. Current molecular medicine. 2008; 8:481–491. [PubMed: 18781955]

Uhlen M, Fagerberg L, Hallstrom BM, Lindskog C, Oksvold P, Mardinoglu A, Sivertsson A, Kampf C, Sjostedt E, Asplund A, et al. Proteomics. Tissue-based map of the human proteome. Science (New York, NY). 2015; 347:1260419.

Wang L, Li HG, Xia ZS, Wen JM, Lv J. Prognostic significance of erythropoietin and erythropoietin receptor in gastric adenocarcinoma. World journal of gastroenterology : WJG. 2011; 17:3933–3940. [PubMed: 22025882]

Wu SY, Yang X, Gharpure KM, Hatakeyama H, Egli M, McGuire MH, Nagaraja AS, Miyake TM, Rupaimoole R, Pecot CV, et al. 2'-OMe-phosphorodithioate-modified siRNAs show increased loading into the RISC complex and enhanced anti-tumour activity. Nature communications. 2014; 5:3459.

Zamora DO, Davies MH, Planck SR, Rosenbaum JT, Powers MR. Soluble forms of EphrinB2 and EphB4 reduce retinal neovascularization in a model of proliferative retinopathy. Investigative ophthalmology & visual science. 2005; 46:2175–2182. [PubMed: 15914639]

HIGHLIGHTS

- EphB4 functions as a canonical Epo receptor
- rhEpo-mediated EphB4 activation triggers downstream signaling *via* STAT3
- rhEpo induces EphB4-mediated functional and biological effects
- EphB4 expression negatively correlates with clinical outcome

Significance

The mechanisms underlying the adverse effects of Epo stimulating agents on reduced survival of cancer patients are not well understood. Herein, we identified EphB4 as an alternative Epo receptor, which triggers Src/Stat3 signaling *via* EphB4. We also showed that rhEpo-mediated tumor growth can be abrogated by targeting EphB4 *in vivo*. In our study, evaluation of human ovarian and breast cancer samples revealed that EphB4, but not the canonical EpoR, correlated with clinical outcome in Epo-treated patients. Overall, we present converging evidence from *in vitro*, *in vivo*, and clinical studies that EphB4 is a critical mediator of Epo-induced cancer growth. Our study provides an important and clinically significant dimension to the biology of erythropoietin.

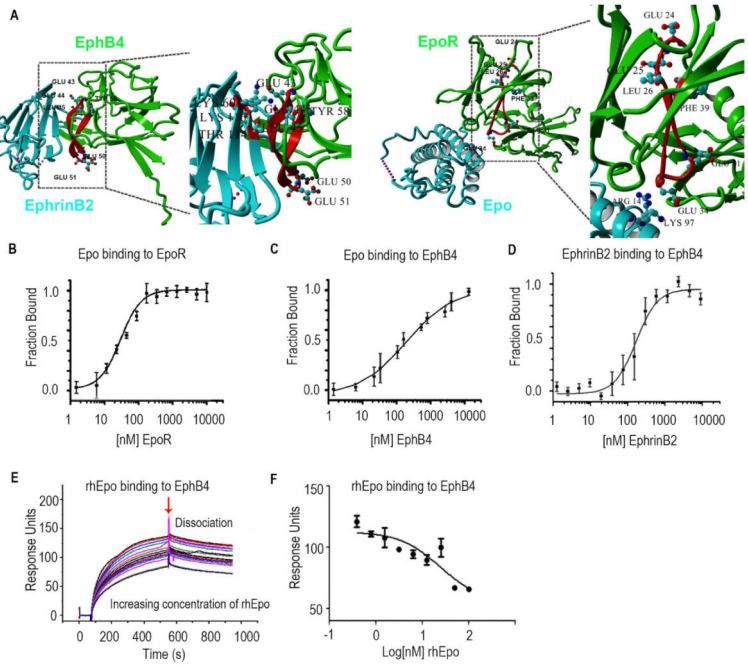

Figure 1. Epo Binds to EphB4

(A) X-ray crystal structure of EphB4 (green), EphrinB2 (blue) and Epo (blue) -EpoR (green) complex. The C-D region from which the inhibitory peptide has been derived from is highlighted in red. E43, E44 and L45 are involved in EphrinB2 binding. Interactions between homology region with EpoR and ligand are shown in detail: E43, E44 and L45 of EphB4 interact with K60, T114 and K116 of EphrinB2. The acidic residues in the apical position of the loop (E50, E51) are shown as well. The A-B loop region homologous to the inhibitory peptide is highlighted in red. Interaction between K97 and R14 of Epo with acidic residue located on the apical loop of the homology region (E34). The region homologous to EphB4 ranges from E24, E25, L26 to F39. E24, E25 and L26 of EpoR are homologous to residues E43, E44 and L45 of EphB4 which are involved in Ephrin ligand binding. Acidic residues are located in the loop in an apical position similar to the location of acidic residues in the A-B loop region of Epo Receptor. **(B)** Fluorescence microscale thermophoresis analysis of Epo binding to EpoR or **(C)** EphB4. **(D)** EphrinB2 binding to labeled EphB4. **(E)** Surface competition assay (SCA) of Epo and EphrinB2 with coated EphB4 receptor using the BIAcore instrument for detection of bound protein. Serial dilutions of Epo were mixed with EphrinB2 and injected onto a CM5 chip to which EphB4 was bound. **(F)** Bound protein shown as response units (RU) at the end of association was plotted as a function of Epo concentration and fit with a three-parameter non-linear regression using Graphpad Prism 5.0. Samples and a buffer blank were injected in duplicate. Mean ± SEM values are shown. (n=3). (See also Figure S1).

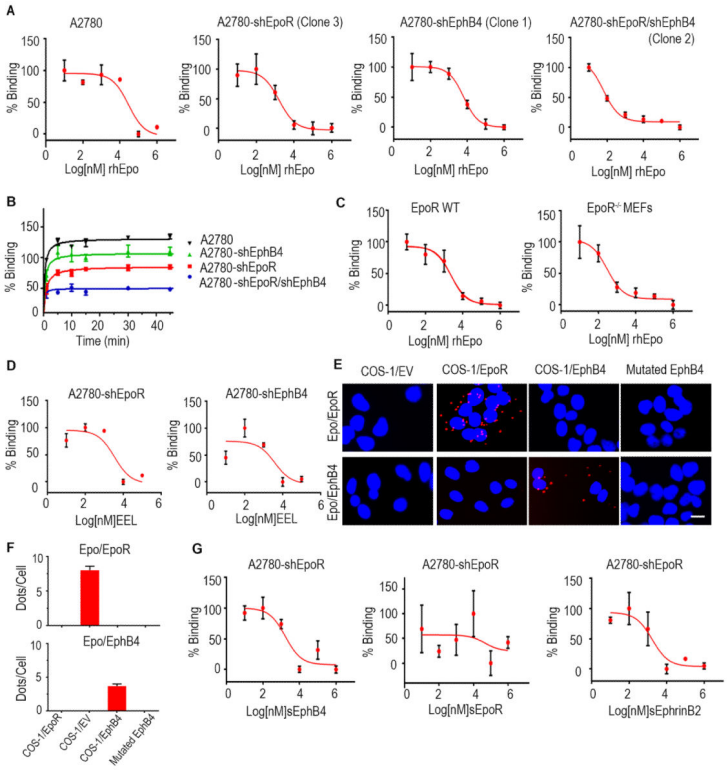

Figure 2. Characterization of rhEpo binding to EphB4 cells

(A) Analysis of competitive binding of [I^{125}]rhEpo to A2780-parental, -shEpoR, -shEphB4, and shEpoR/shEphB4 cells. **(B)** Kinetics of [I^{125}]rhEpo binding to A2780-parental, -shEpoR, -shEphB4, and -shEpoR/shEphB4 cells. **(C)** Analysis of competitive binding of [I^{125}]rhEpo to EpoR WT and EpoR$^{-/-}$ MEFs. **(D)** Competitive binding studies using the EEL peptide in A2780-shEpoR or -shEphB4 cells. **(E)** Proximity ligation assay using Cos-1EpoR, Cos-1EphB4, and mutated EphB4 cells. Scale bar represents 50 μm. **(F)** Bar graph represents the quantification of ligation assay. **(G)** Competitive binding studies using soluble EphB4, EpoR or EphrinB2 in A2780-shEpoR cells. CPM, counts per minute. Mean ± SEM values are shown. (n=3). (See also Figure S2 and Table S1-S2).

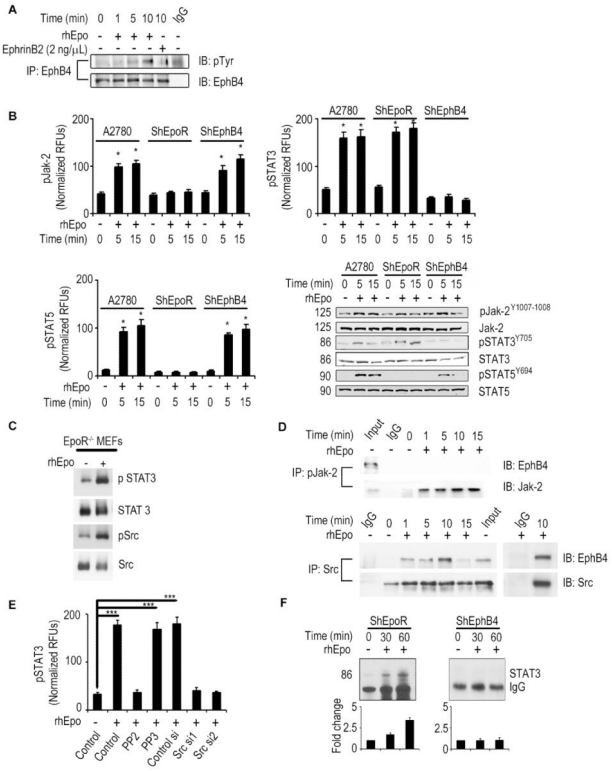

Figure 3. Epo binding to EphB4 activates the Src-STAT pathway

(A) Activation of EphB4 by rhEpo in A2780-parental cells. **(B)** Evaluation of pJak-2, pSTAT5, and pSTAT3 levels (ELISA and Western blot) following rhEpo treatment in A2780, -shEpoR, and -shEphB4 cells. **(C)** Evaluation of pSTAT3 levels following rhEpo treatment in EpoR$^{-/-}$ MEFs. **(D)** Effect of rhEpo on EphB4 binding to Jak-2 and Src in A2780-EpoR cells. **(E)** Effect of Src inhibitor (PP2, 10μM; inactive counterpart, PP3) or Src siRNA on pSTAT3 levels following treatment with rhEpo in A2780-shEpoR cells, (RFUs - relative fluorescence units), n=3. **(F)** Effect of rhEpo on STAT3 binding to a oligonucleotide containing consensus STAT3 binding site in A2780-shEpoR and -shEphB4 cells. Dose of rhEpo used for these experiments was 50 IU/mL. Mean ± SEM values are shown. *$p < 0.05$; ***$p < 0.001$. (See also Figure S3).

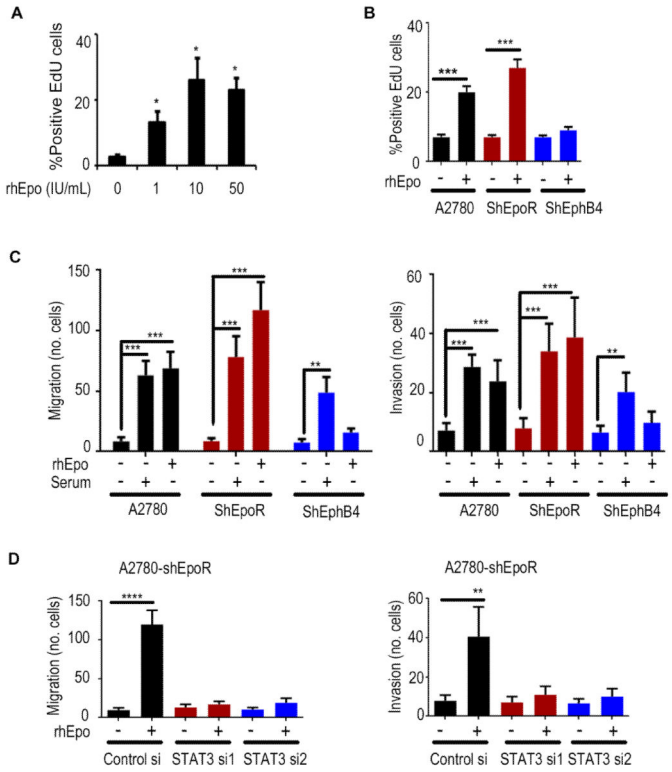

Figure 4. An essential role of EphB4 in rhEpo-mediated effects on cancer cells

(A) Effect of rhEpo on proliferation at indicated dosage. **(B)** Proliferation, **(C)** migration, and invasion of A2780, -shEpoR, and -shEphB4 cells after rhEpo treatment. **(D)** Effect of STAT3 silencing on migration and invasion in A2780-shEpoR cells. Mean ± SEM values are shown. *p < 0.05; **p < 0.01; ***p <0.001; ****p <0.0001. n=3. (See also Figure S4).

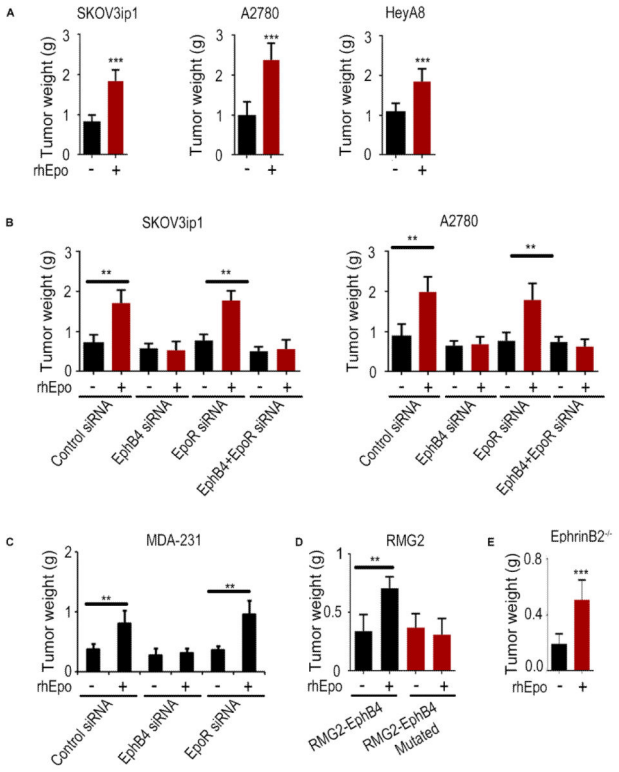

Figure 5. EphB4 plays a key role in Epo-induced tumor growth *in vivo*

(A) Effect of rhEpo (50 IU given 3x/week i.p; n=10) on tumor growth (aggregate tumor weight after 3-5 weeks of rhEpo treatment) in orthotopic ovarian cancer models *in vivo*. **(B)** Effect of EphB4 and EpoR silencing on SKOV3ip1 and A2780 tumor growth *in vivo* with or without rhEpo treatment (n=10). Effect of EphB4 or EpoR silencing on the MDA-231 tumor growth *in vivo* with or without rhEpo treatment (n=10). **(D)** Effect of ectopically expressed EphB4 or EphB4 mutant on RMG2 tumor growth *in vivo* with or without rhEpo treatment (n=10). **(E)** Effect of rhEpo (50 IU given 3x/week i.p; n=10) on ID8-VEGF tumor growth (aggregate tumor weight after 3-5 weeks of rhEpo treatment; 1×10^6 ID8-VEGF murine ovarian cancer cells were injected into EphrinB2$^{-/-}$ mice). Mean ± SEM values are shown. **p < 0.01; ***p <0.001. (See also Figure S5).

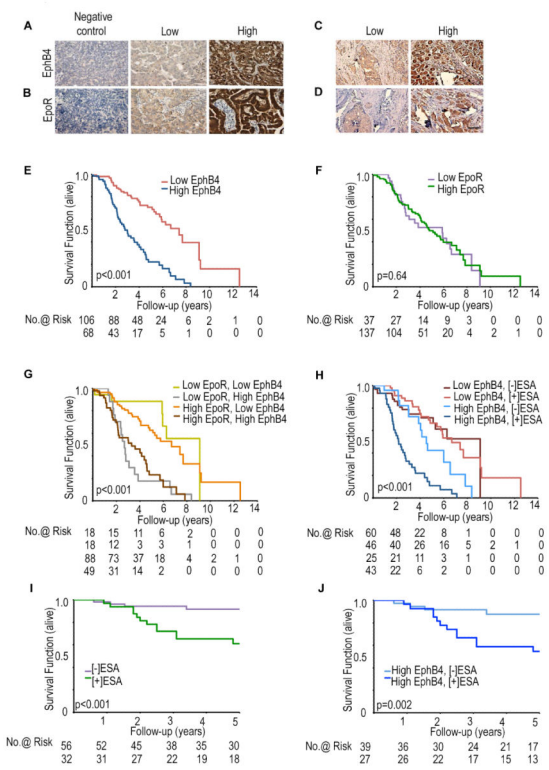

Figure 6. Clinical relevance of EphB4 and EpoR expression and ESA treatment in cancer patients

Representative immunohistochemical-peroxidase staining for **(A)** EphB4 and **(B)** EpoR expression in ovarian cancer, and **(C)** EphB4 and **(D)** EpoR expression in breast cancer samples. Kaplan-Meier curves of disease-specific mortality for ovarian **(E-H)** and breast **(I-J)** cancer patients stratified by tumoral expression of **(E)** EphB4, **(F)** EpoR, or **(G)** both EphB4 and EpoR. **(H)** Evaluation of disease-specific survival duration of ovarian cancer patients based on ESA-treatment and EphB4 expression; **(I)** Disease-specific survival analysis of breast cancer patients stratified by ESA treatment; **(J)** Disease-specific survival of breast cancer patients based on ESA treatment and EphB4 expression. Scale bar represents 50 μm. (See also Figure S6 and Table S3-S7).

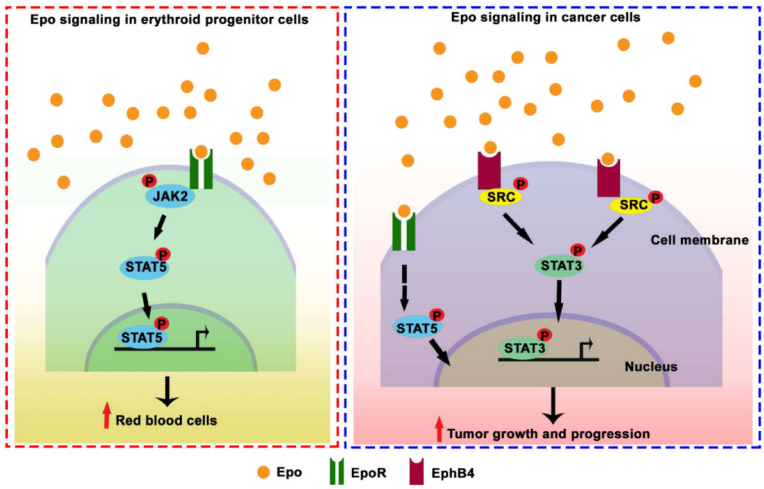

Figure 7.
Proposed model of Epo mediated EphB4 signaling in cancer cells.